Meyer-Neldel rule in charge-trapping metastability in *p*-type hydrogenated amorphous silicon

Richard S. Crandall
National Renewable Energy Laboratory, Golden, Colorado 80401
(Received 13 December 2001; revised 13 June 2002; published 15 November 2002)

Measurements of capacitance transients due to charge-carrier emission from metastable defects in *p*-type hydrogenated amorphous silicon (*a*-Si:H) *p*/*n* junction structures show that both holes and electrons can be metastably trapped in the *p* layer. At 350 K electrons and holes are emitted at the same rate, thereby defining the isokinetic temperature (T_{iso}) for the Meyer-Neldel rule. The enthalpy changes for hole and electron emission are 0.94 and 0.51 eV, respectively. Charge emission rates are measured above and below T_{iso}. The entropy changes for hole and electron emission are 31 and 17 Boltzmann constants, respectively. Below T_{iso} electrons are emitted faster than holes, and above T_{iso} the reverse is true. These relative changes in emission rates are a direct consequence of the large entropy changes in the defect reactions. T_{iso} within experimental error, is the same as the H glass equilibration temperature (360 K) measured by others in *p*-type *a*-Si:H. Arguments are presented suggesting that the defect reactions measured here are involved in H glass equilibration.

DOI: 10.1103/PhysRevB.66.195210 PACS number(s): 61.43.Dq, 73.61.Jc

I. INTRODUCTION

A. Aims

Previous measurements of metastable-defect annealing kinetics in doped hydrogenated amorphous silicon (*a*-Si:H) showed that both majority and minority carriers can be metastably trapped in either boron or phosphorous-doped films.[1] These results were obtained using junction capacitance measurements on *p*/*n* or *n*/*p* structures to measure the emitted charge. A typical device is held at some reverse bias and then a brief forward bias pulse at elevated temperature injects charge into the doped layer under investigation. This charge injection produces metastably trapped electrons and holes. By plotting the logarithm of the characteristic emission time for electrons and holes versus the reciprocal temperature (an Arrhenius plot), straight lines are obtained, and from their slope the activation energy for defect annealing is determined in boron-doped *a*-Si:H. These lines are not parallel, and their extrapolation suggested that they would intersect at about 360 K. This intersection at a finite temperature suggested that this metastable system obeyed the Meyer-Neldel rule (MNR) or compensation law as this type of behavior is also called.[2] The intersection defines the isokinetic temperature (T_{iso}); nevertheless from the limited experimental data it is not at all clear that the characteristic emission times will follow the straight line extrapolations all the way down to 360 K. Furthermore it is a question of deep scientific interest whether the emission times will continue to follow the same straight lines on the Arrhenius plot below T_{iso}. In the present study I show that this is indeed the case. The measurements determine both the enthalpy and entropy changes for the two reactions. In addition I suggest how these defect reactions control dopant equilibration.

B. Background

1. Meyer-Neldel rule

The large body of literature amassed since its discovery in 1937 attests to the widespread applicability of the Meyer-Neldel rule. This rule connects the activation energy (E_{act}) in a family of thermally activated processes with the prefactor in the expression

$$r = \nu_0 e^{-E_{act}/k_B T}, \tag{1}$$

where r is some variable that is activated, T is the temperature, and k_B is the Boltzmann constant. ν_0 and E_{act} are connected by the MNR:

$$\ln(\nu_0) = a + bE_{act}, \tag{2}$$

with a and b positive constants. The slope of Eq. (2) defines T_{iso} by $b^{-1} = k_B T_{iso}$. All $r(T_{iso})$ are the same in the MNR family. In these equations ν_0 would be an attempt-to-escape frequency. However, we see that ν_0 can vary by many orders-of magnitude.

The MNR is obeyed in many transport processes in solids and liquids. It has been observed in systems as diverse as liquid semiconductors[3] and protein denaturation.[4] In many instances where the MNR is obeyed the activation energy is much greater than the highest system excitation (phonons) energy. Perhaps the first systematic observation of this rule was in diffusion in crystalline solids where it was given the name the ''compensation law.''[5] The term ''compensation'' certainly represents the essential physics since the law means that the increase in ν_0 with E_{act} compensates for the Boltzmann factor in reaction (1). There have been various attempts to explain Eq. (2). See Refs. 6 and 7 for a discussion of the different approaches. Perhaps the most satisfying are the models based on the realization that there is considerable entropy associated with the assembly of a large number of system excitations (phonons) together at a particular site to make a thermally activated jump over a barrier.[6–8]

2. Meyer-Neldel rule in amorphous silicon

Many properties of hydrogenated-amorphous silicon (*a*-Si:H) such as: diffusion,[9] conductivity,[10] and metastable defect (MSD) annealing rates[11] exhibit a MNR behavior. The literature contains many examples of annealing of metasta-

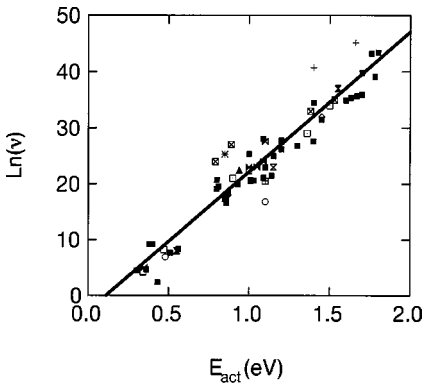

FIG. 1. Logarithm to the base *e* of the attempt-to-escape frequency vs. activation energy for annealing of metastable changes in a variety of *a*-Si:H structures from Ref. 11. The symbols are explained in the reference.

bilities in *a*-Si:H. See, for example, Ref. 11 and references therein. These metastable effects include; the well known Staebler-Wronski effect where transport properties degrade following strong illumination,[12] metastable charge-trapping,[13] quenched-in defects,[14,15] and photo induced structural changes.[16] In many cases detailed annealing studies determined the defect annealing kinetics and from these the annealing activation energy ($E_{\rm act}$) and attempt-to-escape frequency (ν).[12–14,17] In 1991 I collected the then-available data for annealing of light-induced and charge trapping induced metastable changes as well as quenched-in defects and plotted them as $\ln(\nu)$ vs $E_{\rm act}$. $E_{\rm act}$ varied from 0.3 to 1.8 eV for measurements on doped and undoped films and devices. Figure 1 shows a MNR plot for *a*-Si:H taken from Ref. 11. Although there is considerable scatter in the data, a $T_{\rm iso} \approx 490$ K is determined from the line in Fig. 1.[11] At the time it appeared that there was a single $T_{\rm iso}$ characterizing *a*-Si:H. However, this is not the case and the actual situation is that $T_{\rm iso}$ for doped and undoped *a*-Si:H are different, as shown in the present work. The data in Fig. 1 are determined from the a large family of defect annealing reactions all of which were analyzed for $E_{\rm act}$ and ν obtained by an extrapolation of the log (τ) versus 1/temperature line to infinite temperature. However, there could be smaller families of reactions with a slightly different $T_{\rm iso}$ that would not be apparent because the data in Fig. 1 are heavily weighted by the large number of measurements on undoped *a*-Si:H. Only by measuring emission rates above and below $T_{\rm iso}$ can its value be uniquely determined.

3. Defect equilibration in amorphous silicon

The Xerox group[14,18,19] put considerable effort into studying quenched-in metastable effects in doped *a*-Si:H, and proposed the ''hydrogen glass model'' of MSD equilibration. They found that rapidly quenching a sample of doped *a*-Si:H from elevated temperature resulted in an increase in the conductivity, and thus the number of active dopants. The changes are not permanent but anneal with increasing rate as an equilibration temperature ($T_{\rm equ}$) is approached from below. They argued that above $T_{\rm equ}$, the states that control the electronic conductivity are in equilibrium. $T_{\rm equ}$ depends on the dopant type, it is 403 and 363 K for *n*- and *p*-type doping, respectively.[14,18,19] They argued that the temperature at which H freely moves through the material and mediates MSD equilibration determines $T_{\rm equ}$. In addition they suggested that annealing (recovery) kinetics were determined by hydrogen diffusion, being faster in *p*-type than in *n*-type *a*-Si:H. They further showed that annealing followed a Kohlrausch[20] or stretched-exponential time dependence, modeling the annealing kinetics in terms of dispersive hydrogen motion.[21] However, it was shown later that this model was not unique and did not prove that H was involved in defect equilibration.[11,22] Nevertheless Branz and Iwaniczko[23] demonstrated that $T_{\rm equ}$ did indeed vary in the predicted manner with the H diffusion constant by measuring a series of samples of varying H content. Stutzmann[24] showed that quenching *n*-type samples above $T_{\rm equ}$ results in an increase in the density of active dopants. So it seems clear that defect equilibration in doped *a*-Si:H results in dopant activation or deactivation. Furthermore, McMahon and Tsu found that $T_{\rm equ} = 473$ K in undoped amorphous silicon.[15] Thus for both undoped and *p*-type $T_{\rm iso}$ and $T_{\rm equ}$ appear to be about the same. In this paper I will suggest a reason why these two temperatures are similar.

4. Metastable defects in amorphous silicon

The annealing transients of metastable defects obey a stretched-exponential time dependence irrespective of the mode of production or detection. Usually their presence is detected by measuring their effect on some property of *a*-Si:H such as changes in the conductivity or solar cell efficiency. If their presence is monitored by capacitance, as in this work, then they are referred to as charge-trapping defects because a charge change is observed to accompany their anneal. Presumably the defects monitored by different methods are the same. For example, annealing metastable defects in solar cells can be monitored by changes in solar cell properties as well as capacitance. Both methods give the same annealing curves.[13] Therefore, in this paper I use charge emission and defect annealing to mean the same phenomenon.

My co-workers and I previously used isothermal capacitance transients to probe charge-trapping defect annealing in *a*-Si:H.[1,13,25] In solar cells either light or carrier injection produced holes or electrons trapped metastably in the *i* layer.[13] Although the annealing activation energy depends on the sample, holes always have the higher activation energy and anneal (emit the charge) slower.[1] All these measurements were made *below* $T_{\rm iso}$. In doped material I also found that both signs of carrier can be trapped in the same layer above $T_{\rm iso}$.[1] However, these measurements showed the surprising result that the carrier with the *higher* activation energy is emitted quicker than the carrier with the lower activation energy. This contradictory result is a property of the MNR rule for measurements made *above* the predicted isokinetic temperature. In this paper I show that, *below* $T_{\rm iso}$ the normal behavior for thermal emission is observed, with the carrier with the lower activation energy being emitted fastest. The reason for this behavior is discussed in this paper.

C. Outline

Section II describes the details of sample preparation and measurement technique. Section III presents results of production and annealing of metastable defects. Section IV discusses the results and shows the MNR behavior for charge emission data above and below T_{iso}. I summarize the results in Sec. V.

II. EXPERIMENT AND DETAILS

A. Sample preparation

The *a*-Si:H junction devices used in this study are fabricated using plasma-assisted chemical-vapor deposition of silane and doping gases. Trimethylboron (TMB) and phosphine, respectively, are used for the *p*- and *n*-type doping. The general device structure is stainless steel substrate/n^+ layer/*i* layer/p^- layer/p^+ layer/*T*CO.

The n^+ and p^+ layers are typically 20 nm thick, and the p^- layer is about 4000 nm. A 5–10-nm-thick undoped layer is deposited between the p^- and n^+ layers to avoid excess reverse bias leakage because a p/n junction is a high conductance recombination junction. Either TCO or Pd top contacts to the p^+ layer restrict the sample area to 0.05 cm^2. The doping gas concentrations in SiH_4 are 0.4% TMB for the p^+ layer and 0.5% PH_3 for the n^+ layer. This procedure produces a good Ohmic contact to the lightly doped layer. For the p^- layer, the TMB/SiH_4 ratio in the gas phase is 0.00016.

B. Measurement technique

To determine the charge trapped on metastable defects, I apply the familiar junction-capacitance method.[26] The capacitance is measured using a lock-in amplifier (Stanford Instruments Model 850) at a frequency of 10 kHz and an ac test voltage of 0.03 V rms. The device is mounted on a heated sample holder capable of maintaining a stable temperature (+/−1 K) between 299 and 600 K. As described above, the samples consist of thin heavily doped *a*-Si:H layers and a much thicker lightly doped *p* layer. Therefore, changes in the depletion width (W_D) due to changes in the applied bias voltage occur in the lightly doped *p* layer. The measured capacitance ($C \propto 1/W_D$) reflects the electronic processes near the edge of the depletion width at its intersection with the *p* layer bulk.

Figure 2 is a schematic of a majority carrier emission transient following charge injection into the depleted region. Trapped charge initially causes a decrease in the capacitance owing to neutralization of some of the original depletion charge. With time the trapped charge is emitted and $C(t)$ approaches $C(-0)$, the initial capacitance. Using the depletion width approximation,[26] the trapped charge, $N(t)$, is related to the capacitance by

$$N(t) \propto |\Delta C^2(t)| = |C^2(t) - C^2(-0)|. \tag{3}$$

For minority carrier emission, the transient is positive rather than negative as it is for majority carrier emission (Fig. 2).

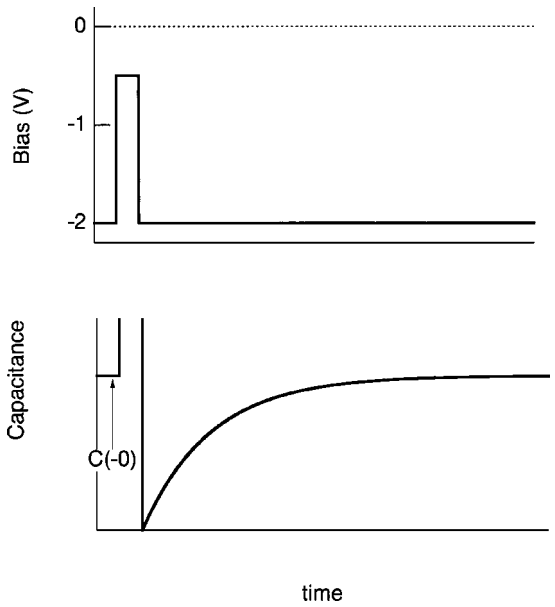

FIG. 2. A sketch of a bias pulse and the resulting capacitance transient for majority carrier emission. $C(-0)$ is the capacitance just before applying the bias pulse.

As previously discussed,[25,27,28] majority carrier emission transients measured in the vicinity of room temperature exhibit an entirely different character from those measured at elevated temperature that are presumably due to emission from metastable defects. Capacitance transients (for short filling pulses) representing hole emission from a dangling bond follow a fast power-law decay and are virtually temperature independent. This behavior is observed for holes[27] in lightly doped *p*-type matures electrons in lightly doped *n*-type material.[29] Charge emission from a MSD is best described by a stretched-exponential function of the form:

$$N(t) = N_{\mathrm{Met}} e^{-(1/\tau_{\mathrm{Met}})^{\alpha}}, \tag{4}$$

exhibiting a strong temperature dependence. N_{Met} is the original number density of metastably trapped charge, τ_{Met} their relaxation time and α the dispersion constant which is $0 < \alpha < 1$.[29] Furthermore, the emission time from dangling bonds follows a linear scaling law with the injection time,[27] whereas the charge emission time from a MSD follows a logarithmic scaling with the injection time and N_{Met} increases rapidly with increasing temperature. In this paper I will show only the slower transients described by Eq. (4).

1. Isothermal degradation

Capacitance transients can be obtained in either an isothermal or heat-quench mode. In the isothermal mode one applies a reverse bias of, for example, −1 V, and waits until the capacitance reaches a steady value $C(-0)$. The bias voltage is then increased to inject charge for 0.1 ms–1000 s, permitting previously depleted regions to fill with charge. This charge is captured by either existing defects or may produce new ones in the mobility gap. After abruptly switching the bias back to its original value of −1 V, the charge carriers in shallow traps are immediately swept out, whereas

charge trapped by metastable defects is thermally emitted on a much slower time scale producing the observed transient.

A difficulty with isothermal degradation is that both the magnitude of the capacitance change and the emission time of the charge transient depend weakly on the degradation time.[25] Since at lower temperatures a longer degradation time is necessary to give a measurable charge emission transient, the emission transients may not be representative of the same starting conditions as those at elevated temperature. This is especially true for minority carriers since they must diffuse over a high potential barrier into the depletion width. This behavior skews an Arrhenius plot of emission time versus reciprocal temperature.[25] Therefore I will use a variation of the heat-quench method used by the Xerox group to measure metastable relaxation.[14]

2. Heat-quench method

Prior to each measurement the sample is equilibrated at the measurement temperature and bias (V_{rev}) until the initial capacitance attains a steady value. Then the temperature is raised to about 480 K for 10 min at forward bias (V_{for}) and then cooled to the measurement temperature at a rate of about 5 K/min. The time at 480 K is long enough for all the defects to equilibrate. This equilibration procedure is similar to that used by the Xerox group.[21] However, the cooling procedure used in the present junction devices is slower. Because the bias remains forward of the measuring bias during cooling, charge that is emitted is not swept out of the junction and has a chance to be re-trapped metastably during cooling. When the temperature is stable, the bias is then changed to V_{rev} to measure the charge emission transient. Any charge that was emitted during cooling and did not recombine is immediately swept out of the junction and is not observed in the transient.

III. EXPERIMENTAL RESULTS

This section describes results of measurements of defect annealing and its analysis. All measurements are made on *p*-type *a*-Si:H between 310 and 475 K.

A. Above T_{iso}

Figure 3 shows a capacitance transient measured in a typical heat-quench cycle. Holes are injected into the depletion region during the equilibration phase at 0 V. Some are trapped metastably and widen the depletion width decreasing the capacitance. During the charge emission phase at -2 V, the depletion width returns to its original value as the injected holes are emitted. The solid curve through the data points is a stretched-exponential function. The data do not show any minority carrier (electron) trapping and subsequent emission because the equilibration bias is only 0 V. At this V_{for}, few electrons surmount the potential barrier from the n^+ into the p^- layer. However, increasing V_{for} lowers the potential barrier for injection and produces a measurable electron emission transient.

Figure 4 is an example of a transient that shows that both holes and electrons can be metastably trapped in the same material layer. The sample is the same as shown in Fig. 3. However, $V_{rev}=0$ V and $V_{for}=0.5$ V. Initially $\Delta C^2(t)<0$ showing that more holes than electrons are trapped in the depletion width. Later, $\Delta C^2(t)$ increases as the trapped holes are emitted. However, $\Delta C^2(t)$ overshoots zero because the depletion width still contains trapped electrons that are emitted later than the holes. Note that if the electrons were trapped in the n^+ layer they would give a majority carrier transient with $\Delta C^2(t)<0$. Thus they must be trapped in the p^- layer. Finally $\Delta C^2(t)$ returns to 0 as all the charge is finally emitted. The dashed lines representing the two stretched-exponential decays used to fit the data also show that at the shortest times about 50% more holes are trapped than electrons. For these transients the minority carrier electron is emitted nearly 100 times *slower* than the hole.

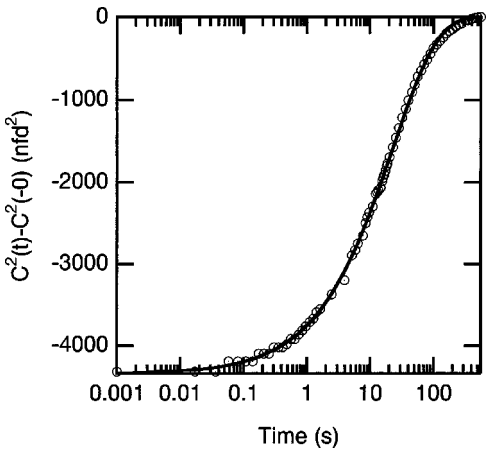

FIG. 3. A capacitance transient measured at -2-V bias at 429 K after quenching from 480 K at 0 V. The solid line through the data points is the fit of a stretched exponential function showing hole emission. The fitting parameters are $\tau_{Met}=22.5$ s and $\alpha=0.6$.

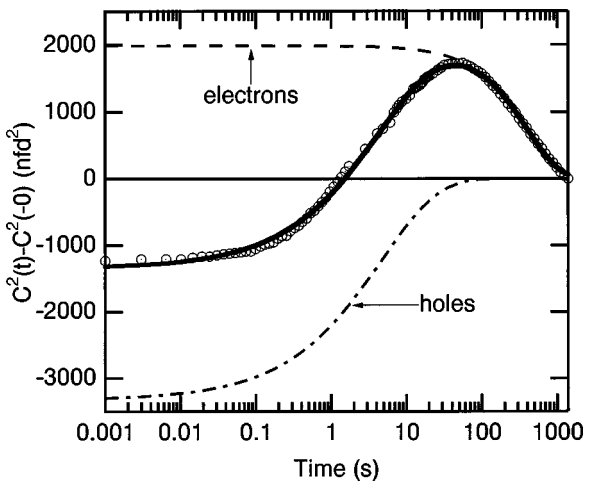

FIG. 4. A capacitance transient measured at 0-V bias at 427 K quenched from 480 K at 0.5 V. The solid line through the data points is the combined fit of the two stretched exponential functions shown by dashed and dot-dash lines. $\tau_{Met}=4.7$ and 403 s for holes and electrons, respectively.

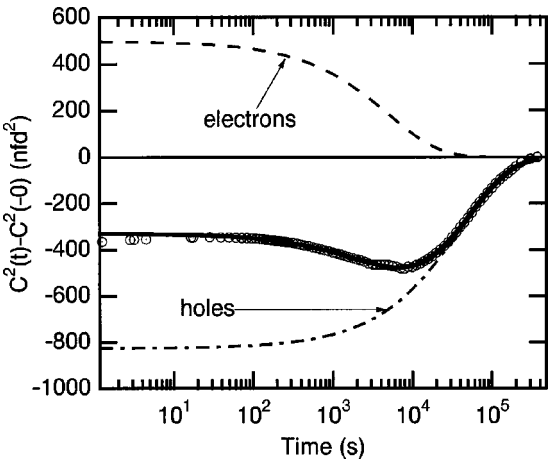

FIG. 5. Capacitance transient measured at 0-V bias at 313 K quenched from 480 K at 0.5 V. The solid line through the data points is the combined fit of the two stretched exponential functions shown by dashed and dot-dashed lines. $\tau_{\mathrm{Met}}=46000$ and 5500 s for holes and electrons, respectively.

B. Below T_{iso}

Figure 5 shows an emission transient at lower temperature with the same heat-quench cycle as used for the data in Figs. 3 and 4. Initially $\Delta C^2(t)<0$ showing that more holes than electrons are again trapped in the depletion width. First, in contrast to Fig. 4, $\Delta C^2(t)$ begins to decrease as *electrons* are emitted before any holes are emitted. Finally, $\Delta C^2(t)$ returns to zero as holes are emitted. For these data obtained at lower temperature than those in Fig. 3, the hole emission time as lengthened more than the electron emission time. This transient at 313 K is just the opposite of what is observed at 427 K. At the higher temperature the majority carrier was emitted first and now the minority carrier is emitted first.

Figure 6 shows an Arrhenius plot of $\log(\tau_{\mathrm{Met}})$ versus reciprocal temperature for both electron and hole emission. The slope of each line determines the activation energy for emission of the trapped carrier from the defect. The intercept of the line with the infinite temperature point gives ν_0.

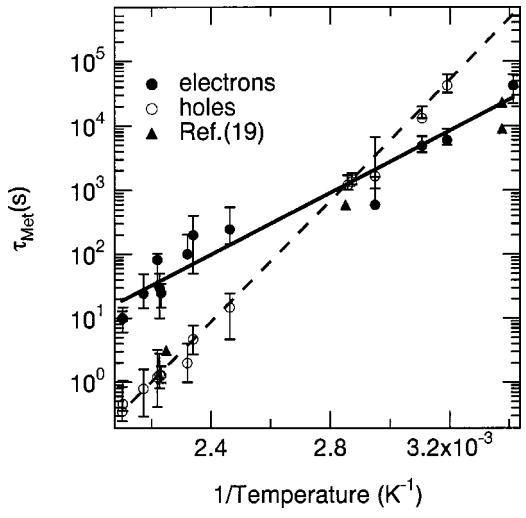

FIG. 6. Charge emission times for holes and electrons vs reciprocal temperature. $T_{\mathrm{iso}}=350$ K. The lines are fits to the data points. $E_{\mathrm{act}}=0.94$ and 0.51 eV for holes and electrons, respectively. $\nu_0=2.4\times10^{10}$ and 15 000 s^{-1} for holes and electrons, respectively. The triangles are from Ref. 19.

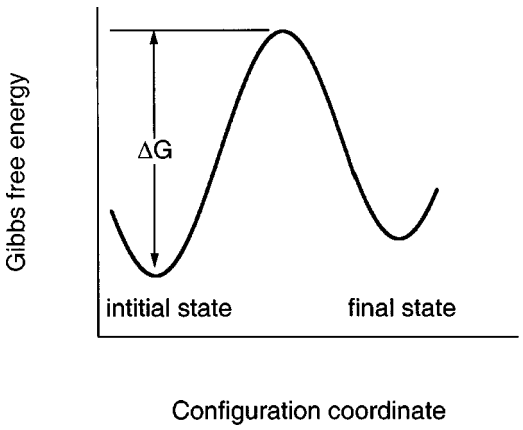

FIG. 7. Sketch of the Gibbs free energy change for hole and electron emission vs temperature.

IV. DISCUSSION

The data presented in Fig. 6 clearly show that charge emission from metastable defects in *a*-Si:H obeys the MNR. This example of measurements showing charge carrier emission above and below T_{iso} gives an unambiguous determination of T_{iso}. Usually measurements are made only below T_{iso}. Thus to determine T_{iso} one must extrapolate a series of Arrhenius plots for different samples to a point where all the lines would cross to define T_{iso}. Sometimes this procedure can introduce sizable errors in the determination of T_{iso} because the extrapolation is over a large temperature. The lines in Fig. 6 cross at a unique point giving a value of $T_{\mathrm{iso}}\approx350$ K. Furthermore they show τ_{Met} extending over a large region on either side of T_{iso}.

To correctly describe these charge emission transitions we must treat the defects as thermodynamic objects and use the Eyring theory[30] to calculate the reaction rate r for a transition over a potential barrier. Figure 7 is a schematic showing a typical transition from an initial state over a potential barrier to a final state. Only the transition to the top of the barrier governs the reaction rate since it is assumed that the transition across the barrier top is so fast that it does not affect the overall rate. In this theory r is given by

$$r=\tau_{\mathrm{Met}}^{-1}=\nu_{00}e^{-\beta\Delta G}=\nu_{00}e^{(\Delta S/k_B)}e^{-\beta\Delta H}, \tag{5}$$

where $\Delta G=\Delta H-T\Delta S$ is the difference in Gibbs free energy between the initial state and the top of the activation barrier for the transition. ΔH and ΔS are, respectively, the enthalpy and the entropy of the defect, $\beta=1/k_BT$, and ν_e the Eyring constant given by $\nu_e=k_BT/h$, with h the Plank constant. The change in enthalpy (ΔH) is equivalent to the emission activation energy E_{act}.

For the present system the reaction rates for both hole and electron transitions are equal at T_{iso}. This requires the ΔG for each transition to be the same at T_{iso}, in turn requiring

that $(\Delta S_h - \Delta S_e)T_{\rm iso} = (\Delta H_h - \Delta H_e)$. The subscripts refer to the hole and electron, respectively. In fact, this is a general result for a family of reactions such as those studied here. It may be stated that a family of reactions obeys the MNR if and only if the ratio $(\Delta H_1 - \Delta H_2)/(\Delta S_1 - \Delta S_2) > 0$ at some finite temperature. $T_{\rm iso}$ is equal to this ratio. Using this general result and forming the ratio of transition rates for a pair of reactions, r_1 and r_2, using Eq. (5), gives

$$\frac{r_1}{r_2} = e^{-\beta(\{\Delta H_1 - \Delta H_2\}[1-(T/T_{\rm iso})])}. \tag{6}$$

Equation (6) clearly shows why the ratio of the pair of emission rates goes through unity and a particular transition changes from faster to slower at $T_{\rm iso}$; the transition with the larger ΔH is faster for $T > T_{\rm iso}$ and slower for $T < T_{\rm iso}$, as shown in Fig. 6. Note that the opposite situation is not possible.

It is straightforward to find that the individual entropy changes. The MNR states that r is independent of ΔH at the isokinetic temperature. To have this condition there must be an entropy term that is proportional to ΔH and of the correct sign so that the coefficient of ΔG in Eq. (5) is zero at $T = T_{\rm iso}$. This term must be $\Delta S = \Delta H / T_{\rm iso}$. There could be, however, additional entropy terms that do not depend on ΔH. Thus the measured entropy changes are

$$\Delta S_h = 31 k_B, \quad \Delta S_e = 17 k_B.$$

These large ΔS values lend support to the model that ΔS represents the number of ways that the necessary number of phonons, n, required to surmount the potential barrier can be assembled.[7,8] Assuming an Einstein model gives $n = \Delta H / E_p$ where E_p is the maximum phonon energy. A simple argument[7] gives

$$\frac{\Delta S}{k_B} = \ln\left[\frac{N!}{n!(N-n)!}\right],$$

where N is the number of phonons in the interaction volume. For want of a better value, I determine E_p from the peak of a typical Raman scattering spectrum in a-Si:H, giving $E_p \approx 0.06$ eV.[31] Thus n is about 16 and 9 and N is 24 and 16 for holes and electrons, respectively. As expected, the number of phonons in the interaction volume is greater than n supporting the original conjecture.

The above results and discussion are independent of the nature of the MSD. However, it would be useful to speculate on the nature of this defect in p-type a-Si:H. Either two distinct or a single defect could explain my data.

It is tempting to make the simplest interpretation to the data. That is that a hole is trapped on a neutral dangling bond and an electron on a positively charged dangling bond. This explanation does not seem likely from what is known about hole trapping and emission from a neutral dangling bond as[27] as discussed in Sec. II. Perhaps the best feature to distinguish between charge emission from dangling bond and a MSD is that there is a temperature and time dependent barrier for charge trapping by the MSD,[13] but not for charge trapping on the dangling bond.[25] A short (10^{-4} s) charge injection pulse is sufficient to fill all the dangling bonds. This time is apparently independent of temperature. Metastable defects are filled (or formed) slowly with injection pulse time.[25]

Thus it does not seem possible that charge trapping by isolated dangling bonds can explain the results presented here. However, this does not rule out trapping by dangling bonds that are part of a molecular complex. The MSD measured in this work is most likely a complex of two or more atoms. In the following I discuss the main features that a MSD needs to explain the data presented above.

Branz[32] discussed a variety of charge-trapping reactions that might explain the MSD involved in defect equilibration. These reactions all involve a bond switching which would present a potential barrier for MSD formation or destruction. It seems possible that this kind of reaction might be involved in the reactions involved in this paper.

The simplest type of MSD consistent with experiment would be amphoteric. The bistable charge-trapping reactions involving two atoms and charge emission and bond rearrangement sketched below might govern MSD production and capture:

$$M_b^{q+1} + X_c \Leftrightarrow M_{b*}^{q} + X_{c*} + h^+ \tag{7a}$$

and

$$M_{b*}^{q-1} + X_{c*} \Leftrightarrow M_b^{q} + X_c + e^-, \tag{7b}$$

where M is some atom whose charge q changes in the reaction and X a neighboring atom that switches a bond with M. The subscripts b and c are integers representing coordination numbers. As reaction (7a) goes to the right M reduces its charge by unity and a hole is emitted. The reverse of this reaction is hole capture that occurs during the injection phase. M and X either reform the bond or break their bond. The reaction can go to the left and capture a hole to form the MSD. Similar arguments hold for reaction (7b). To proceed further requires an assumption of the actual defect involved in Eqs. (7).

One can speculate that the defect involved in the present experiment is that involved in dopant equilibration where it is believed that the principal dopant is activated by quenching above the equilibration temperature. If this were the case then my experiment would probe the characteristic times involved in this process. Making this assumption Eqs. (7) can be rewritten in terms of the dopant (boron) to give the following pair of reactions:

$$B_3^0 + X_{c*} \Leftrightarrow B_4^- + X_c + h^+ \tag{8a}$$

and

$$B_4^- + X_c \Leftrightarrow B_3^0 + X_{c*} + e^-, \tag{8b}$$

where X would be a Si or a Si containing complex that could bond to the B when the dopant is activated. This complex could contain an H in analogy with the model for dopant activation in n-type Si.[33] In steady state these reactions would proceed in both directions to introconvert the two charge states of boron.

Let the density of B_4^- and B_3^0 that changes in reaction (8) be ΔB_4^- and ΔB_3^0, respectively. Furthermore I assume that the number of B involved in reaction (8) remains constant at the value $B_{ex}=\Delta B_3^0+\Delta B_4^-$. Then the rate equation governing dopant activation or deactivation is

$$\frac{d\Delta B_4^-}{dt}=\Delta B_3^0 r_h-\Delta B_4^- r_e \tag{9}$$

and $d\Delta B_4^-/dt=0$ in the steady state. Combining Eqs. (9) and (6) one obtains:

$$\frac{\Delta B_4^-}{\Delta B_3^0}=\frac{r_h}{r_e}=e^{-\beta(\Delta H_h-\Delta H_e)[1-(T/T_{iso})]}. \tag{10}$$

Equation (10) shows the essential result that T_{iso} separates the region of excess dopant activation from the region of excess dopant destruction. During charge injection at $T \gg T_{equ}, T_{iso}$, hole emission, reaction (8a), is much faster than electron emission producing an excess of B_4^-. Below T_{iso} the opposite situation applies, giving an excess of B_3^0.

Equation (9) is readily solved to describe how the system approaches the steady state following a disturbance. For example, the annealing of excess dopant $[\Delta B_4^-(0)]$ is described by

$$\Delta B_4^-(t)=\Delta B_4^-(0)e^{-(r_h+r_e)t}+\frac{r_h}{(r_h+r_e)} \times \Delta B_{ex}(1-e^{-(r_h+r_e)t}), \tag{11}$$

with the quantity $(r_h/(r_h+r_e))\Delta B_{ex}$ giving the steady-state density of ΔB_4^-. Equation (11) shows that in an annealing measurement the fastest reaction will dominate the annealing time.

Similarly the increase in excess dopant due to a disturbance, such as rapidly increasing the temperature is given by the expression

$$\Delta B_4^-=B_{ex}\frac{r_h}{r_e+r_h}(1-e^{-t(r_e+r_h)}). \tag{12}$$

Note that in both Eqs. (11) and (12) that the characteristic time is $\tau_c=\tau_h\tau_e/(\tau_h+\tau_e)$.

If the reactions measured here are indeed those that govern defect equilibration, then the emission times measured here should be roughly those measured in equilibration measurements.[19] That this is indeed the case is seen in Fig. 6, where the triangles are the characteristic times for annealing of excess dopants in *p*-type *a*-Si:H taken from Ref. 19. These data agree quite closely with the charge emission data measured in the present work. The dopant annealing timesare slightly faster than τ_{Met} presumably because of the higher doping density for the equilibration measurements.[19] Above T_{iso} the equilibration times are governed by the time to *increase* the density of bandtail holes. Below T_{iso} the equilibration is determined by the time to *decrease* the bandtail holes. This is the reaction [Eq. (8b)] that produces electrons (destroys) holes. If this were not the case and the annealing time for excess dopants were determined by the hole producing reaction (8a) then the annealing time would have be over an order of magnitude slower than the measured value. These results suggest why T_{equ} is so close to T_{iso}. Both defect equilibration and charge emission are governed by the same reactions.

V. SUMMARY

This paper shows that it is possible to measure metastable trapped-carrier emission (defect annealing) both above and below the isokinetic temperature in the same sample. This is possible because in doped *a*-Si:H it is possible to simultaneously trap holes and electrons on metastable defects and also that T_{iso} is low enough to permit measurements above T_{iso}. Surprisingly, each sign of charge has its own annealing activation energy (charge emission rate). Measuring the charge emission rates of both electrons and holes between 313 and 480 K permits an unequivocal determination of the isokinetic temperature ($T_{iso}=350$ K). The enthalpy changes for hole and electron emission are 0.94 and 0.51 eV and the entropy changes are 31 and 17 Boltzmann constants, respectively. Below T_{iso} electrons are emitted faster than holes, and above T_{iso} the reverse is true. These relative changes in emission rates are a direct consequence of the large entropy changes in the emission reactions.

ACKNOWLEDGMENTS

I am indebted to Arthur Yelon for many discussions of the Meyer-Neldel Rule, Howard Branz for helpful discussions on dopant equilibration, Yueqin Xu for growing the junction devices, and Martin Carlen for discovering minority carrier emmision MSD. The U.S. Department of Energy supported this work, under Contract No. DE-AC36-83CH10093.

[1] R. S. Crandall, J. Non-Cryst. Solids **266–269**, 423 (2000).
[2] W. Meyer and H. Neldel, Z. Tech. Phys. **12**, 588 (1937).
[3] J. Fortner, V. G. Karpov, and M. Saboungi, Appl. Phys. Lett. **66**, 997 (1995).
[4] B. Rosenberg, G. Kemeny, R. C. Switzer, and T. C. Hamilton, Nature (London) **37**, 1425 (1971).
[5] R. W. Keyes, J. Chem. Phys. **29**, 467 (1958).
[6] A. Yelon and B. Movaghar, Phys. Rev. Lett. **65**, 618 (1990).
[7] A. Yelon, B. Movaghar, and H. M. Branz, Phys. Rev. B **46**, 12 244 (1992).
[8] E. Peacock-Lopez and H. Suhl, Phys. Rev. B **26**, 3774 (1982).
[9] J. Shinar, R. Shinar, X. L. Wu, S. Mitra, and R. F. Girvan, Phys. Rev. B **43**, 1631 (1991).
[10] X. Wang, Y. Bar-Yam, D. Adler, and J. D. Joannopoulos, Phys. Rev. B **38**, 1601 (1988).
[11] R. S. Crandall, Phys. Rev. B **43**, 4057 (1991).
[12] D. L. Staebler and C. R. Wronski, Appl. Phys. Lett. **31**, 292 (1977).

[13] R. S. Crandall, Phys. Rev. B **36**, 2645 (1987).
[14] R. A. Street, J. Kakalios, and T. M. Hayes, Phys. Rev. B **34**, 3030 (1986).
[15] T. J. McMahon and R. Tsu, Appl. Phys. Lett. **51**, 412 (1987).
[16] H. Fritzsche, Solid State Commun. **94**, 953 (1995).
[17] M. Stutzmann, W. B. Jackson, and C. C. Tsai, Appl. Phys. Lett. **45**, 1075 (1984).
[18] J. Kakalios and R. A. Street, Phys. Rev. B **34**, 6014 (1986).
[19] R. A. Street, M. Hack, and W. B. Jackson, Phys. Rev. B **37**, 4209 (1988).
[20] F. Kohlraush, Ann. Phys. (Leipzig) **12**, 393 (1847).
[21] J. Kakalios, R. A. Street, and W. B. Jackson, Phys. Rev. Lett. **59**, 1037 (1987).
[22] V. Halpern, Phys. Rev. Lett. **67**, 611 (1991).
[23] H. M. Branz and E. Iwaniczko, in *Amorphous Silicon Technology–1992*, edited by A. Madan, M. J. Thompson, P. G. LeComber, Y. Hamakawa, and P. C. Taylor, MRS Symposia Proceedings No. 258 (Materials Research Society, Pittsburgh, 1992), p. 389.
[24] M. Stutzmann, Phys. Rev. B **35**, 9735 (1987).
[25] R. S. Crandall and M. W. Carlen, J. Non-Cryst. Solids **190**, 133 (1995).
[26] G. L. Miller, D. V. Lang, and L. C. Kimerling, Annu. Rev. Mater. Sci. **7**, 377 (1977).
[27] M. W. Carlen, Y. Xu, and R. S. Crandall, Phys. Rev. B **51**, 2173 (1995).
[28] R. S. Crandall *et al.*, in *Amorphous Silicon Technology—1995*, edited by M. Hack, E. A. Schiff, A. Madan, M. Powell, and A. Matsuda, MRS Symposia Proceedings No. 337 (Materials Research Society, Pittsburg, 1995), p. 897.
[29] J. D. Cohen, T. M. Leen, and R. J. Rasmussen, Phys. Rev. Lett. **69**, 3358 (1992).
[30] S. Glasstone, K. J. Laidler, and H. Eyring, *The Theory of Rate Processes* (McGraw-Hill, New York, 1941).
[31] J. S. Lannin, J. Non-Cryst. Solids **141**, 233 (1992).
[32] H. M. Branz, Phys. Rev. B **38**, 7474 (1988).
[33] E. Z. Liu and W. E. Spear, J. Non-Cryst. Solids **137**, 245 (1991).